

We are IntechOpen, the world's leading publisher of Open Access books Built by scientists, for scientists

6,900

Open access books available

185,000

International authors and editors

200M

Downloads

Our authors are among the

154

Countries delivered to

TOP 1%

most cited scientists

12.2%

Contributors from top 500 universities



WEB OF SCIENCE™

Selection of our books indexed in the Book Citation Index
in Web of Science™ Core Collection (BKCI)

Interested in publishing with us?
Contact book.department@intechopen.com

Numbers displayed above are based on latest data collected.
For more information visit www.intechopen.com



"Impulsar": New Application for High Power High Repetition Rate Pulse-Periodic Lasers

V.V. Apollonov

Prokhorov General Physics Institute RAS, Vavilov str., 38, Moscow, 119991, Russia

1. Introduction

Since the 1970s, the possibility of using a laser engine to launch light satellites into orbit has been attracting the attention of researchers [1-9]. The solution of problems considered in [3] is still of current interest. This is an increase in the efficiency - the coupling coefficient J_r of using laser radiation (the ratio of the propulsion to the radiation power) by several times and the prevention of the shock damage of the apparatus, which appears when high-power repetitively pulsed laser radiation with low repetition rates / is used. For example, for $J_r \sim 0.3 \text{ kN MW}^{-1}$ (this value is typical for an air-jet laser engine of 1970th), the mass of 200 kg, and the acceleration of 10g, the required laser power should be $\sim 60 \text{ MW}$ (the energy $Q \sim 100 \text{ g}$ in the TNT equivalent, $f \sim 100 \text{ Hz}$), and the power of a power supply should be 0.5-1 GW. However, it seems unlikely that such a laser will be created in the near future. In our experiments, $J_r \sim 1 \text{ kN MW}^{-1}$ (obtained experimentally) and $3\text{-}5 \text{ kN MW}^{-1}$ (estimate, special conditions), which allows us to reduce the laser power by a factor of 7-10. A power of 10-15 MW can be obtained already at present with the help of gas-dynamic lasers and HF/DF lasers by using the properties of repetitively pulsed lasing with high repetition rates and methods for power scaling of lasing [10, 11], checked already for CO₂, HF and Nd YAG. .

To solve these problems, it was proposed to use repetitively pulsed radiation with $f \sim 100 \text{ kHz}$, the optical pulsating discharge (OPD), and the effect of merging of shock waves produced by the OPD [12-14]. The merging criteria were confirmed in experiments [15]. The OPD is laser sparks in the focus of repetitively pulsed radiation, which can be at rest or can move at high velocities [16-20]. The high-frequency repetitively pulsed regime is optimal for continuously-pumped Q-switched high-power lasers. In this case, the pulse energy is comparatively small and the stationary propulsion is possible.

The aim of our work is to verify experimentally the possibility of using pulse-periodic laser radiation with a high repetition rate to produce very effective stationary propulsion in a laser jet engine and to demonstrate the advantages of this technology for production of super long conductive canal for energy delivery from space.

2. Experimental

In the model considered in [12-14], the pulsed and stationary regimes are possible. Figure 1 explains the specific features of these regimes. An OPD is produced at the focus of a lens on the axis of a gas jet flowing from a high-pressure chamber or an air intake to a cylindrical

reflector. The shock waves generated by the OPD merge to form a quasi-stationary wave - the high-pressure region between the OPD and reflector.

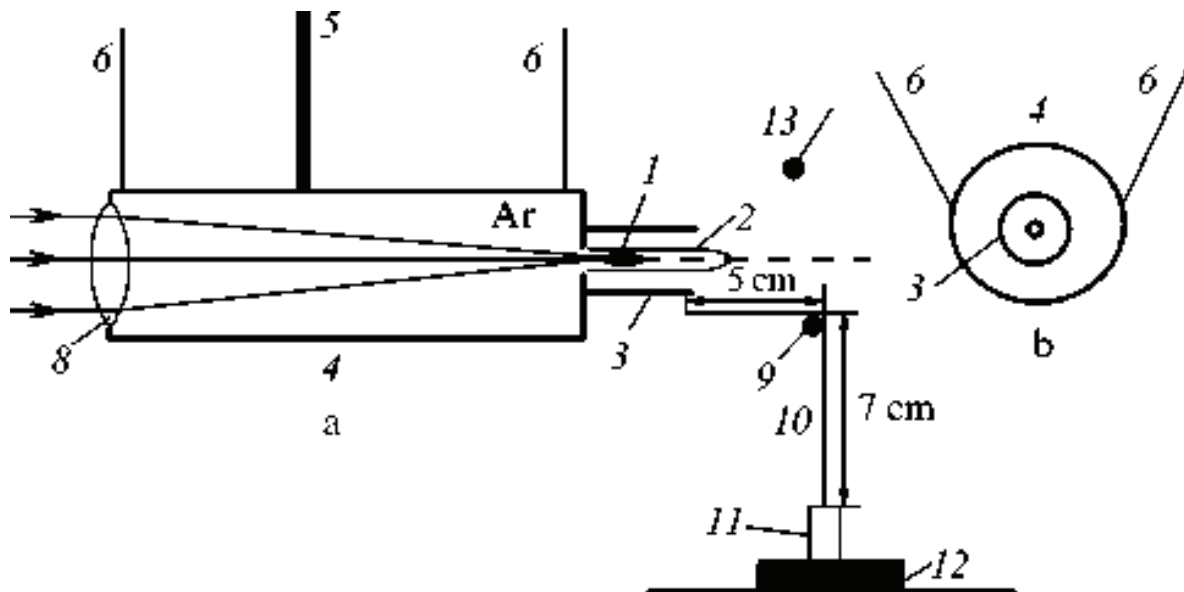


Fig. 1. Scheme of the experiment, side (a) and front (b) view: (1) OPD; (2) argon jet; (3) replaceable cylindrical attachment (reflector); (4) high-pressure chamber (rocket model); (5) elastic hose for argon supply; (6) model suspension wires; (7) laser radiation; (8) focusing lens; (9) block; (10) wire connecting cylinder (3) with weight (11); (12) balance; (13) shock-wave pressure gauge.

As a result, the propulsion F_r appears. In a cylindrical reflector, the coupling coefficient is maximal, $J_r = 1.1 \text{ NkW}^{-1}$ [13], as for a plane explosion [21]. In the pulsed regime, the OPD is produced by trains of laser pulses. A narrow jet of diameter $D_j \sim 0.3R_d$ [13], which is smaller than the reflector diameter D_r , carries a plasma out from the OPD region, which is necessary for the efficient formation of shock waves. Here, $R_d = 2A_5(q/P_0)^{1/3}$ is the dynamic radius of a spark, q (in J) is the laser pulse energy absorbed in a spark, and P_0 (in atm) is the gas pressure. The propulsion acts during a pulse train, whose duration is limited by the air heating time. The hot atmospheric air is replaced by the cold air during the interval between pulses. In the stationary regime, gas continuously arrives to the reflector from the bottom, by forming a jet over the entire section. In experiments in this regime, we have $D_j \sim 2R_d \sim 3 \text{ mm}$, which is comparable with the reflector diameter $D_r \sim 5 \text{ mm}$.

The scheme of the experiment is shown in Figure 1. The OPD was produced by radiation from a pulsed CO_2 laser. The pulse duration was $\sim 1 \mu\text{s}$, the duration of the front peak was $0.2 \mu\text{s}$. The pulse repetition rate was varied from 7 to 100 kHz, the pulse energy was 0.1-0.025 J. The peak power was 300-100 kW, the average power of repetitively pulsed radiation was $W = 600 - 1700 \text{ W}$, and the absorbed power was $W_a = \eta W$ ($\eta \approx 0.7$). Figure 2 shows the shapes of the incident pulse and the pulse transmitted through the OPD region. Note that for a short pulse duration and high power, $\eta \sim 0.95$. Because the radiation intensity at the focus is lower than the optical breakdown threshold in air, the argon jet was used. The length l of sparks along the flow was $\sim 0.5 \text{ cm}$.

The model of a rocket with a laser engine was a duralumin cylinder of diameter $\sim 8 \text{ cm}$, length $\sim 26 \text{ cm}$, and weight 1.1 kg, which was suspended on four thin wires of length 1.1 m and capable of moving only in the axial direction. A reflector (replaceable cylindrical

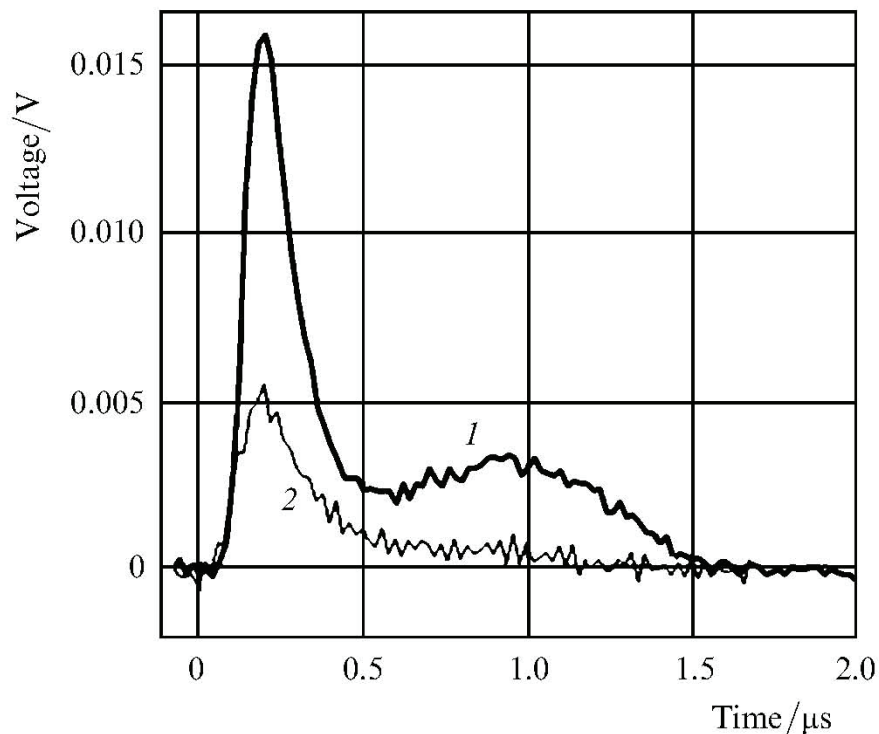


Fig. 2. Oscillograms of the laser pulse (1) and radiation pulse transmitted through the OPD (2) for $f=50$ kHz.

attachment) was mounted on the chamber end. Laser radiation was directed to the chamber through a lens with a focal distance of 17 cm. The argon jet was formed during flowing from a high-pressure chamber through a hole of diameter $\sim 3 - 4$ mm. The jet velocity V was controlled by the pressure of argon, which was delivered to the chamber through a flexible hose. The force produced by the jet and shock waves was imparted with the help of a thin (of diameter ~ 0.2 mm) molybdenum wire to a weight standing on a strain-gauge balance (accurate to 0.1 g). The wire length was 12 cm and the block diameter was 1 cm.

The sequence of operations in each experiment was as follows. A weight fixed on a wire was placed on a balance. The model was slightly deviated from the equilibrium position (in the block direction), which is necessary for producing the initial tension of the wire (~ 1 g). The reading F_m of the balance was fixed, then the jet was switched, and the reading of the balance decreased to F_1 . This is explained by the fact that the rapid jet produces a reduced pressure (ejection effect) in the reflector. After the OPD switching, the reading of the balance became F_2 . The propulsion F_r produced by the OPD is equal to $F_1 - F_2$. The pressure of shock waves was measured with a pressure gauge whose output signal was stored in a PC with a step of ~ 1 μ s. The linearity band of the pressure gauge was ~ 100 kHz. The gauge was located at a distance of ~ 5 cm from the jet axis (see Figure 1) and was switched on after the OPD ignition ($t = 0$). The pressure was detected for 100 ms.

Let us estimate the possibility of shock-wave merging in the experiment and the expected values of F_r and J_r . The merging efficiency depends on the parameters $\omega = fR_d/C_0$ and $M_0 = V/C_0$ ($M_0 < 1$), where C_0 is the sound speed in gas. If the distance from the OPD region to the walls is much larger than R_d and sparks are spherical or their length l is smaller than R_d , then the frequencies characterizing the interaction of the OPD with gas are:

$$\omega_0 \approx 2.5M_0, \quad (1)$$

$$\omega_1 \approx 0.8(1 - M_0), \quad (2)$$

$$\omega_2 \approx 5.9(1 - M_0)^{1.5}. \quad (3)$$

For $\omega < \omega_1$, the shock waves do not interact with each other. In the range $\omega < \omega_1 < \omega_2$, the compression phases of the adjacent waves begin to merge, this effect being enhanced as the value of ω approaches ω_2 . In the region $\omega < \omega_2$, the shock waves form a quasi-stationary wave with the length greatly exceeding the length of the compression phase of the shock waves. For $\omega < \omega_0$, the OPD efficiently (up to $\sim 30\%$) transforms repetitively pulsed radiation to shock waves.

In the pulsed regime the value of M_0 in (1) corresponds to the jet velocity. Because shock waves merge in an immobile gas, $M_0 \approx 0$ in (2) and (3). The frequencies $f=7-100$ kHz correspond to $R_d = 0.88 - 0.55$ cm and $\omega = 0.2 - 1.7$. Therefore, shock waves do not merge in this case. In trains, where the energy of the first pulses is greater by a factor of 1.5-2 than that of the next pulses ($\omega \approx 2$), the first shock waves can merge. The propulsion produced by pulse trains is $F_r = J_r \eta W = 0.3$ N (~ 30 g), where $J_r = 1.1$ N kW⁻¹, $\eta = 0.6$, and $W \sim 0.5$ kW.

In the stationary regime for $M_0 \sim 0.7$, the shock wave merge because $\omega > \omega_2$ ($\omega = 1.8$, $\omega_2 \approx 1.3$). A quasi-stationary wave is formed between the OPD and the cylinder bottom. The excess pressure on the bottom is $\delta P = P - P_0 = 0.54P_0(R_d/r)^{1.64} \approx 0.25 - 0.5$ atm, and the propulsion is $F_r \approx \pi(D_r^2 - D_j^2)\delta P/4 = 0.03 - 0.06$ kg.

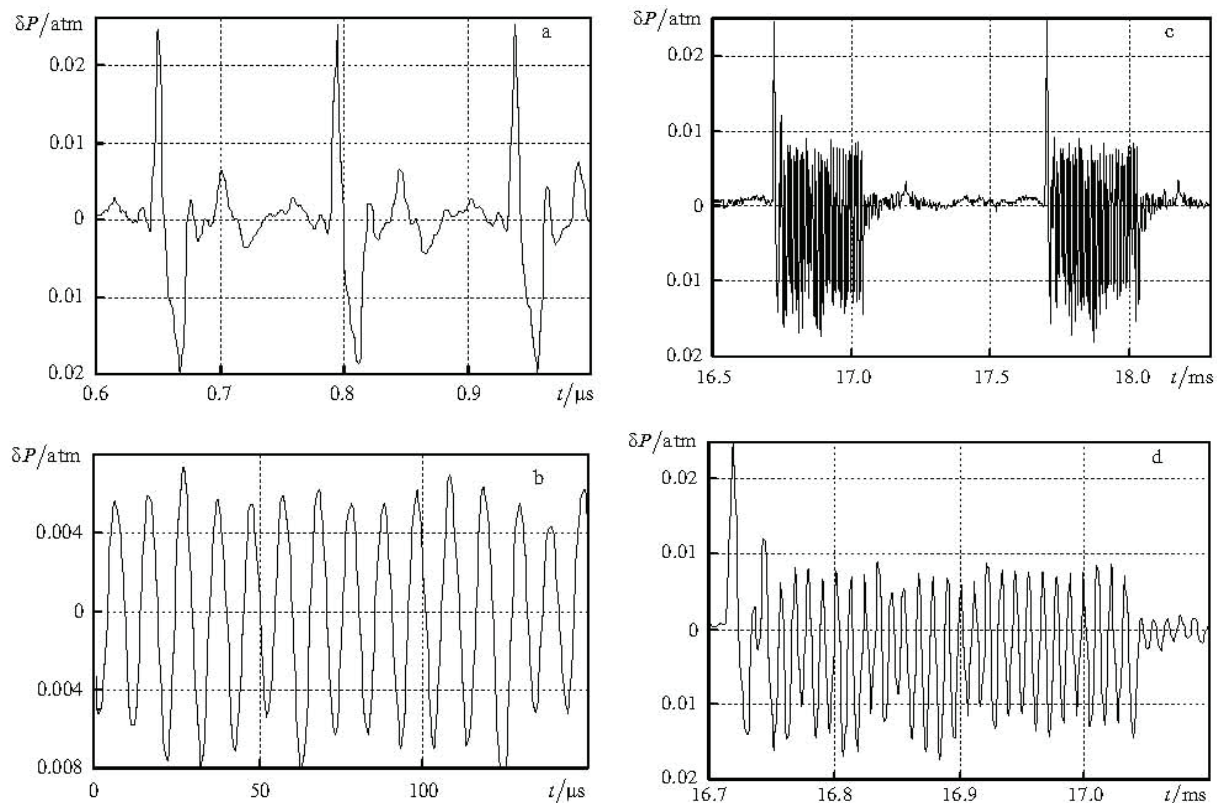


Fig. 3. Pressure pulsations produced by the OPD for $V=300$ ms⁻¹ without reflector), $f=7$ kHz, $W=690$ W (a); $f=100$ kHz, $W=1700$ W (b), and $f=100$ kHz, the train repetition rate $\varphi=1$ kHz, $W=1000$ W, the number of pulses in the train $N=30$ (c); the train of shock waves at a large scale, parameters are as in Fig. 3c (d).

3. Results of measurements

3.1 Control measurements

The jet propulsions F_j and F_r and the excess pulsation pressure $\delta P = P - P_0$ were measured for the model without the reflector. We considered the cases of the jet without and with the OPD. The jet velocity V and radiation parameters were varied. For $V = 50, 100$, and 300 m s^{-1} , the propulsion produced by the jet was $F_j = 6, 28$, and 200 g , respectively, and the amplitude of pulsations was $\delta P = 5 \times 10^{-6}, 2 \times 10^{-5}$ and $3 \times 10^{-4} \text{ atm}$. The OPD burning in the jet did not change the reading of the balance. This is explained by the fact that the OPD is located at a distance of r from the bottom of a high-pressure chamber, which satisfies the inequality $r/R_d > 2$, when the momentum produced by shock waves is small [3, 22]. As follows from Fig. 3, pulsations $\delta P(t)$ produced by the OPD greatly exceed pressure fluctuations in the jet.

3.2 Stationary regime

The OPD was burning in a flow which was formed during the gas outflow from the chamber through a hole ($D_j = 0.3 \text{ cm}$) to the reflector ($D_r = 0.5 \text{ cm}$) (Figure 4). Because the excess pressure on the reflector bottom was $\sim 0.5 \text{ atm}$ (see above), to avoid the jet closing, the pressure used in the chamber was set equal to $\sim 2 \text{ atm}$. The jet velocity without the OPD was $V = 300$ and 400 ms^{-1} , $F_j = 80$ and 140 g . The OPD was produced by repetitively pulsed radiation with $f = 50$ and 100 kHz and the average power $W \approx 1200 \text{ W}$ (the absorbed power was $W_a \approx 650 \text{ W}$). Within several seconds after the OPD switching, the reflector was heated up to the temperature more than 100°C .

Figure 5 illustrates the time window for visualization of shock waves with the Schlieren system in the presence of plasma. Before $7 \mu\text{s}$, the plasma is too bright relative to the LED source, and all information about the shock wave is lost. At $7 \mu\text{s}$, the shock wave image could be discerned under very close examination. By $10 \mu\text{s}$, the shock wave is clearly visible in the image; however, at this time the shock wave has nearly left the field of view. A technique was needed to resolve the shock waves at short timescales, when plasma was present.

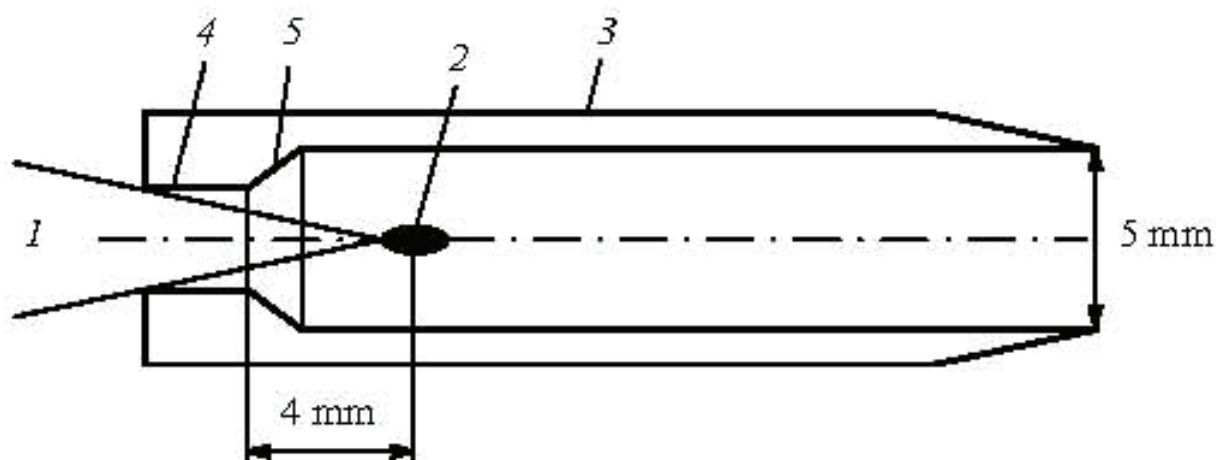


Fig. 4. Reflector of a stationary laser engine: (1) repetitively pulsed laser radiation with $f = 50$ and 100 kHz , $W = 1200 \text{ W}$; (2) OPD; (3) reflector; (4) hole of diameter $\sim 3 \text{ mm}$ through which argon outflows from a high-pressure chamber ($\sim 2 \text{ atm}$) to the reflector; (5) reflector bottom, the angle of inclination to the axis is $\sim 30^\circ$.

For $f = 50$ kHz and $V = 300$ m s⁻¹, the propulsion is $F_r = 40$ g, and for $V = 400$ m s⁻¹ the propulsion is 69 g; the coupling coefficient is $J_r \approx 1.06$ N kW⁻¹. The propulsion F_r is stationary because the criteria for shock-wave merging in front of the OPD region are fulfilled. Downstream, the shock waves do not merge. One can see this from Figure 5 demonstrating pressure pulsations $\delta P(t)$ measured outside the reflector. They characterize the absorption of repetitively pulsed radiation in the OPD and, therefore, the propulsion. For $f = 50$ kHz, the instability is weak (± 5 %) and for $f = 100$ kHz, the modulation $\delta P(t)$ is close to 100 %. The characteristic frequency of the amplitude modulation $f_a \approx 4$ kHz is close to $C_0/(2H)$, where H is the reflector length. The possible explanation is that at the high frequency f the plasma has no time to be removed from the OPD burning region, which reduces the generation efficiency of shock waves. The jet closing can also lead to the same result if the pressure in the quasi-stationary wave is comparable with that in the chamber. Thus, repetitively pulsed radiation can be used to produce the stationary propulsion in a laser engine.

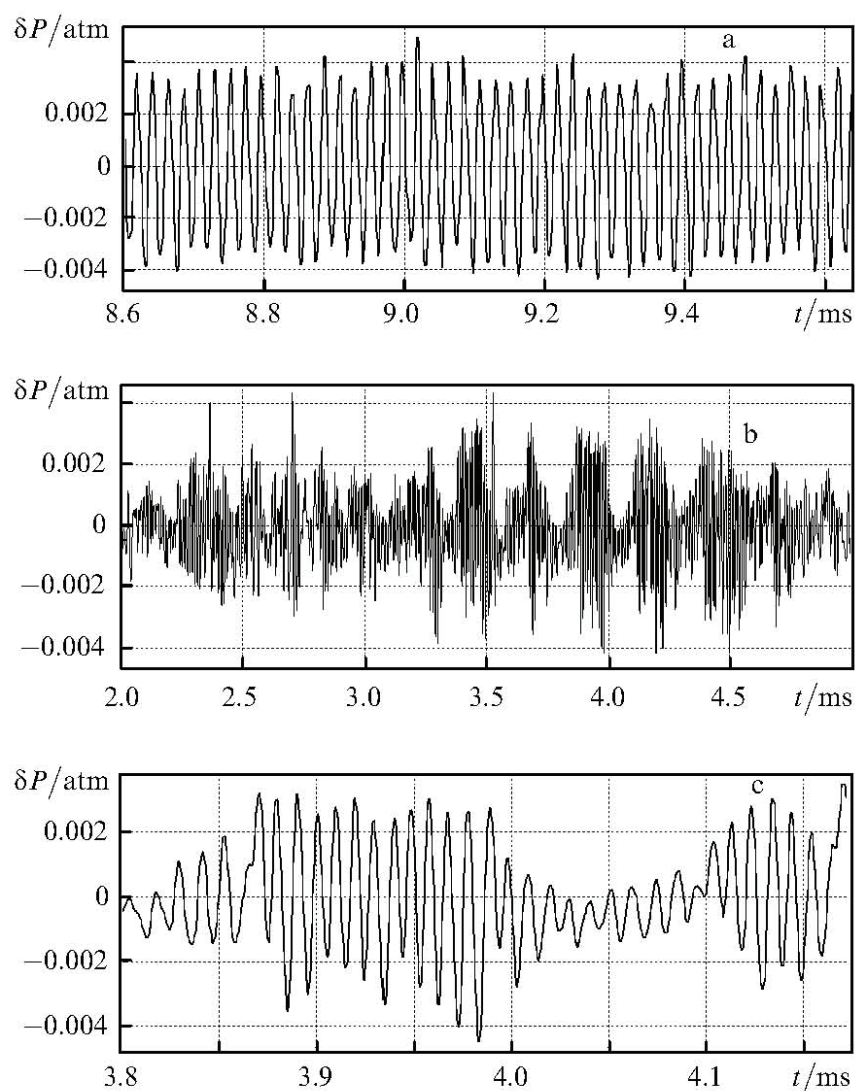


Fig. 5. Pressure pulsations δP produced upon OPD burning in the reflector with $D_r = 0.5$ cm, $H = 4/6$ cm, $V = 400$ m s⁻¹, $D_j = 0/3$ cm for $f = 50$ kHz, $W = 1300$ W (a) and $f = 100$ kHz, $W = 1200$ W (b, c).

3.3 Pulsed regime

To find the optimal parameters of the laser engine, we performed approximately 100 OPD starts. Some data are presented in Table 1. We varied the diameter and length of the reflector, radiation parameters, and the jet velocity (from 50 to 300 m s⁻¹). For $V=50\text{ m s}^{-1}$ the ejection effect is small, for $V=300\text{ m s}^{-1}\approx C_0$, this effect is strong, while for $V\approx 100\text{ ms}^{-1}$, the transition regime takes place. In some cases, the cylinder was perforated along its circumference to reduce ejection. The OPD was produced by radiation pulse trains, and in some cases – by repetitively pulsed radiation. The structure and repetition rate of pulse trains was selected to provide the replacement of the heated OPD gas by the atmospheric air. The train duration was $\sim 1/3$ of its period, the number of pulses was $N=15$ or 30, depending on the frequency f . The heating mechanism was the action of the thermal radiation of a plasma [23], the turbulent thermal diffusivity with the characteristic time $\sim 300\text{ }\mu\text{s}$ [24] and shock waves.

The propulsion F_r was observed with decreasing the reflector diameter and increasing its length. The OPD burned at a distance of $\sim 1\text{ cm}$ from the reflector bottom. One can see from Figure 6 that the shock waves produced by the first high-power pulses in trains merge. For $f=100\text{ kHz}$, the pulse energy is low, which is manifested in the instability of pressure pulsations in trains. As the pulse energy was approximately doubled at the frequency $f=50\text{ kHz}$, pulsations $\delta P(t)$ were stabilized. The OPD burning in the reflector of a large diameter ($D_r/R_d\approx 4$) at a distance from its bottom satisfying the relation $r/R_d\approx 3$ did not produce the propulsion.

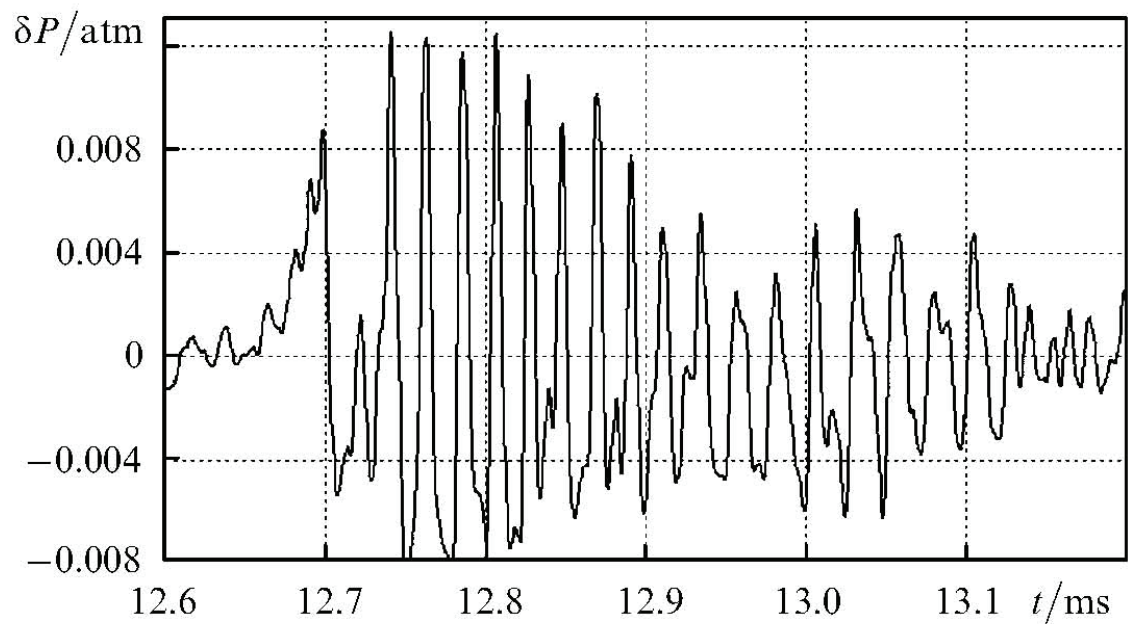


Fig. 6. Pressure pulsations δP in the OPD produced by pulse trains with $\varphi=1.1\text{ kHz}$, $f=50\text{ kHz}$, $W=720\text{ W}$, $N=15$, $V=300\text{ m s}^{-1}$, $D_r=1.5\text{ cm}$, $H=5\text{ cm}$, $D_j=4\text{ mm}$, and $F=4.5\text{ g}$.

Table 1 presents some results of the measurements. One can see that the coupling coefficient J_r strongly depends on many parameters, achieving 1 N kW^{-1} in the stationary regime and 0.53 N kW^{-1} in the pulsed regime.

At present, the methods of power scaling of laser systems and laser engines, which are also used in laboratories, are being extensively developed [10, 25]. Let us demonstrate their

application by examples. We observed the effect when the OPD produced the 'negative' propulsion $F_t = -97 \text{ g}$ (see Table 1), which correspond to the deceleration of a rocket. The value of J_r can be increased by approximately a factor of 1.5 by increasing the pulse energy and decreasing their duration down to $\sim 0.2 \text{ }\mu\text{s}$. An important factor characterizing the operation of a laser engine at the high-altitude flying is the efficiency I_m of the used working gas. The value $I_m = 0.005 \text{ kg N}^{-1}\text{s}^{-1}$ can be considerably reduced in experiments by using a higher-power radiation. The power of repetitively pulsed radiation should be no less than 10 kW. In this case, F_r will considerably exceed all the other forces. The gas-dynamic effects that influence the value of F_r , for example, the bottom resistance at the flight velocity $\sim 1 \text{ km s}^{-1}$ should be taken into account.

f/kHz	φ/kHz	$D_t/\text{mm}, [H/\text{mm}]$	N	$V/\text{m s}^{-1}$	W/W	F_j/g	F_r/g	$J_r/\text{N kW}^{-1}$	Reflector material
45	RP	5, [46]	—	300	1300	80	40	0.61	duralumin
45	RP	5, [46]	—	400	1300	141	69	1.06	— " —
100	RP	5, [46]	—	400	1200	155	54	1.08	— " —
100	1	15, [50]	30	300	720	49	4	0.085	— " —
45	1	15, [50]	15	50	720	0.9	2.1	0.042	— " —
45	1	15, [50]	15	300	720	49.1	4.5	0.09	— " —
45	1	15, [50]	15	50	720	1.2	1.4	0.028	duralumin*
45	1	15, [50]	15	100	720	6.3	5.6	0.11	— " —
45	1	15, [50]	15	300	720	62.7	4	0.08	— " —
45	1	15, [50]	5	170	500	17.7	3.5	0.1	— " —
45	2	15, [50]	5	100	600	6.3	4.8	0.11	— " —
45	2	15, [50]	5	164	600	18.5	7.5	0.18	— " —
45	2	15, [50]	5	300	600	70	—4	0.095	— " —
12.5	RP	25, [35]	—	60	430	2.4	4	0.13	quartz
12.5	RP	25, [35]	—	100	430	5	7	0.23	— " —
12.5	RP	25, [35]	—	150	430	11	11	0.37	— " —
12.5	RP	25, [35]	—	300	430	51	16	0.53	— " —
12.5	RP	25, [35]	—	50	430	6	1	0.033	duralumin**
12.5	RP	25, [35]	—	100	430	12	7	0.23	— " —
12.5	RP	25, [35]	—	300	430	195	—97	—3.2	— " —

Table 1. Experimental conditions and results.

Note. Laser radiation was focused at a distance of 1 cm from the reflector bottom; * six holes of diameter 5 mm over the reflector perimeter at a distance of 7 mm from its exhaust; **six holes of diameter 5 mm over the reflector perimeter at a distance of 15 mm from its exhaust. Thus, our experiments have confirmed that repetitively pulsed laser radiation produces the stationary propulsion with the high coupling coefficient. The development of the scaling methods for laser systems, the increase in the output radiation power and optimization of the interaction of shock waves will result in a considerable increase in the laser-engine efficiency.

4. The impact of thermal action

A laser air-jet engine (LAJE) uses repetitively pulsed laser radiation and the atmospheric air as a working substance [1-3]. In the tail part of a rocket a reflector focusing radiation is located. The propulsion is produced due to the action of the periodic shock waves produced by laser sparks on the reflector. The laser air-jet engine is attractive due to its simplicity and high efficiency. It was pointed out in papers [26] that the LAJE can find applications for launching space crafts if $\sim 100\text{-kJ}$ repetitively pulsed lasers with pulse repetition rates of hundreds hertz are developed and the damage of the optical reflector

under the action of shock waves and laser plasma is eliminated. These problems can be solved by using high pulse repetition rates ($f \sim 100$ kHz), an optical pulsed discharge, and the merging of shock waves [12, 13]. The efficiency of the use of laser radiation in the case of short pulses at high pulse repetition rates is considerably higher. It is shown in this paper that factors damaging the reflector and a triggered device cannot be eliminated at low pulse repetition rates and are of the resonance type.

Let us estimate the basic LAJE parameters: the forces acting on a rocket in the cases of pulsed and stationary acceleration, the wavelength of compression waves excited in the rocket body by shock waves, the radius R_k of the plasma region (cavern) formed upon the expansion of a laser spark. We use the expressions for shock-wave parameters obtained by us. A laser spark was treated as a spherical region of radius r_0 in which the absorption of energy for the time ~ 1 μ s is accompanied by a pressure jump of the order of tens and hundreds of atmospheres. This is valid for the LAJE in which the focal distance and diameter of a beam on the reflector are comparable and the spark length is small. The reflector is a hemisphere of radius R_r . The frequency f is determined by the necessity of replacing hot air in the reflector by atmospheric air.

Let us estimate the excess of the peak value F_m of the repetitively pulsed propulsion over the stationary force F_s upon accelerating a rocket of mass M . It is obvious that $F_s = Ma$, where the acceleration $a = (10-20)g_0 \approx 100 - 200$ m s⁻². The peak value of the repetitively pulsed propulsion is achieved when the shock wave front arrives on the reflector. The excess pressure in the shock wave (with respect to the atmospheric pressure P_0) produces the propulsion $F_j(t)$ and acceleration a of a rocket of mass M . The momentum increment produced by the shock wave is:

$$\delta p_i = \int_0^{1/f} F_1(t) dt \simeq F_a t_a \text{ [N} \cdot \text{s]}. \quad (4)$$

Here, F_a is the average value of the propulsion for the time t_a of the action of the compression phase of the shock wave on the reflector, and $F_m \approx 2F_a$. By equating δp_i to the momentum increment $\delta p_s = F/f = aM/f$ over the period under the action of the stationary propulsion F_s , we find:

$$\Delta = F_m/F_s = 2/(ft_a). \quad (5)$$

The value of Δ , as shown below, depends on many parameters. The momentum increment per period can be expressed in terms of the coupling coefficient J as $\delta p_i = JQ$, where Q [J] is the laser radiation energy absorbed in a spark. The condition $\delta p_i = \delta p_s$ gives the relation:

$$W = aM/J \quad (6)$$

between the basic parameters of the problem: $W = Qf$ is the absorbed average power of repetitively pulsed radiation, and $J \approx 0.0001 - 0.0012$ N s J⁻¹ [3, 13, 26].

The action time of the compression phase on the reflector is $t_a \sim R_c/V$, where $V \approx k_1 C_0$ is the shock-wave velocity in front of the wall ($k_1 \sim 1.2$) and $C_0 \approx 3.4 \times 10^4$ cm s⁻¹ is the sound speed in air. The length R_c of the shock wave compression phase can be found from the relation:

$$\frac{R_c}{R_d} = 0.26 \left(\frac{h}{R_d} \right)^{0.32}. \quad (7)$$

Here, h is the distance from the spark centre to the reflector surface and $R_d \approx 2.15(Q/P_0)^{1/3}$ is the dynamic radius of the spark (distance at which the pressure in the shock wave becomes close to the air pressure P_0). In this expression, R_d is measured in cm and P_0 in atm. The cavern radius can be found from the relation:

$$\frac{R_k}{R_d} = 0.6 \left(\frac{r_0}{R_d} \right)^{0.29} = 0.22 - 0.3 \approx 0.25. \quad (8)$$

The final expression (8) corresponds to the inequality $r_0/R_d < 0.03 - 0.1$, which is typical for laser sparks (r_0 is their initial radius). Let us find the range of P_0 where the two conditions are fulfilled simultaneously: the plasma is not in contact with the reflector surface and the coupling coefficient J is close to its maximum [3, 22, 26]. This corresponds to the inequality $R_k < h < R_d$. By dividing both parts of this inequality by R_d , we obtain $R_k/R_d < h/R_d < 1$, or $0.25 < h/R_d < 1$. As the rocket gains height, the air pressure and, hence, h/R_d decrease. If we assume that at the start ($P_0 = 1$ atm) the ratio $h/R_d = 1$, where h and R_d are chosen according to (2), then the inequality $0.25 < h/R_d < 1$ is fulfilled for $P_0 = 1 - 0.015$ atm, which restricts the flight altitude of the rocket by the value 30 - 40 km ($h = \text{const}$).

The optimal distance h satisfies the relation $h/R_d \approx 0.25b_i$ where $b_i \approx 4 - 5$. By substituting h/R_d into (7), we find the length of the shock-wave compression phase and the time of its action on the reflector:

$$\frac{R_c}{R_d} \approx 0.17b_i^{0.32}, \quad (9)$$

$$t_a = \frac{0.17b_i^{0.32} R_d}{k_1 C_0} = \frac{s_1 Q^{1/3}}{P_0^{1/3}} = \frac{s_1}{P_0^{1/3}} \left(\frac{aM}{Jf} \right)^{1/3}, \quad (10)$$

Where $s_1 = 0.37b_i^{0.32}/(k_1 C_0) \approx 9 \times 10^{-6} b_i^{0.32}$. From this, by using the relation $\Delta = F_m/F_a = 2/(Ft_a)$ we find:

$$\Delta = \frac{2P_0^{1/3}}{s_1 f^{2/3} W^{1/3}} = \frac{2P_0^{1/3} Q^{2/3} J}{s_1 aM} = \frac{2}{s_1 f^{2/3}} \left(\frac{P_0 J}{aM} \right)^{1/3}. \quad (11)$$

Of the three parameters Q , W , and f , two parameters are independent. The third parameter can be determined from expression (6). The conditions $1/f \sim t_a$ and $\Delta \approx 1 - 2$ correspond to the merging of shock waves [12].

The important parameters are the ratio of t_a to the propagation time $t_z = L/C_m$ of sound over the entire rocket length L (C_m is the sound speed in a metal) and the ratio of t_z to $1/f$. For steel and aluminum, $C_m = 5.1$ and 5.2 km s⁻¹, respectively. By using (10), we obtain:

$$U = \frac{t_a C_m}{L} = \frac{s_1 C_m}{L P_0^{1/3}} Q^{1/3}. \quad (12)$$

Here, L is measured in cm and C_m in cm s⁻¹. Expression (12) gives the energy:

$$Q = \frac{35.4P_0}{b_1^{0.96}} \left(U \frac{C_0}{C_m} \right)^3 L^3. \quad (13)$$

From the practical point of view, of the most interest is the case $U > 1$, when the uniform load is produced over the entire length L . If $U < 1$, the acceleration is not stationary and the wavelength of the wave excited in the rocket body is much smaller than L . If also $C_m/f < L$, then many compression waves fit the length L . The case $U \approx 1$ corresponds to the resonance excitation of the waves. Obviously, the case $U \leq 1$ is unacceptable from the point of view of the rocket strength.

By using the expressions obtained above, we estimate Δ , U , and R_k for laboratory experiments and a small-mass rocket. We assume that $b_i = 4$, $J = 5 \times 10^{-4} \text{ N s J}^{-1}$, and $s_1 = 1.4 \times 10^{-5}$. For the laboratory conditions, $M \approx 0.1 \text{ kg}$, $R_r \approx 5 \text{ cm}$, $L = 10 \text{ cm}$, and $a = 100 \text{ m s}^{-2}$. The average value of the repetitively pulsed propulsion F_{IP} is equal to the stationary propulsion, $F_{IP} = F_s = 10 \text{ N}$; the average power of repetitively pulsed radiation is $W = F_{IP}/J = 20 \text{ kW}$, and the pulse energy is $Q_p = W/f$. We estimate the frequency f and, hence, $Q_p \approx Q$ for the two limiting cases.

At the start, $P_0 \approx 1 \text{ atm}$ and the cavern radius R_k is considerably smaller than R_r . Here, as in the unbounded space, the laser plasma is cooled due to turbulent thermal mass transfer. For $Q_p < 20 \text{ J}$, the characteristic time of this process is 2-5 ms [8,9], which corresponds to $f = 500 - 200 \text{ Hz}$. If $R_k \sim R_r$ ($P_0 < 0.1 \text{ atm}$), the hot gas at temperature of a few thousands of degrees occupies the greater part of the reflector volume. The frequency f is determined by the necessity of replacing gas over the entire volume and is $\sim 0.5C_0/R_r - 850 \text{ Hz}$. Let us assume for further estimates that $f = 200 \text{ Hz}$, which gives $Q_p = 100 \text{ J}$. We find from (7) and (8) that $\Delta = 74$ and $U = 3.5$. This means that the maximum dynamic propulsion exceeds by many times the propulsion corresponding to the stationary acceleration. The action time of the shock wave is longer by a factor of 3.5 than the propagation time of the shock wave over the model length. For $P_0 = 1$ and 0.01 atm , the cavern radius is $R_k = 2.5$ and 11.6 cm , respectively.

5. The dynamic resonance loads

Let us make the estimate for a rocket by assuming that $M \approx 20 \text{ kg}$, $R_r \approx 20 \text{ cm}$, $L = 200 \text{ cm}$, and $a = 100 \text{ m s}^{-2}$. The average repetitively pulsed propulsion is $F_{IP} = F_s = 2000 \text{ N}$, the average radiation power is $W = 4 \text{ MW}$, for $f = 200 \text{ Hz}$ the pulse energy is $Q_p = 20 \text{ kJ}$, $\Delta = 12.6$, $U = 1$, $R_k = 14.7$ and 68 cm ($P_0 = 1$ and 0.01 atm), and $F_m = 25.6 \text{ kN} = 2560 \text{ kg}$. One can see that the repetitively pulsed acceleration regime produces the dynamic loads on the rocket body which are an order of magnitude greater than F_s . They have the resonance nature because the condition $U \sim 1$ means that the compression wavelengths are comparable with the rocket length. In addition, as the rocket length is increased up to 4 m and the pulse repetition rate is increased up to 1 kHz , the oscillation eigenfrequency C_m/L of the rocket body is close to f (resonance).

Thus, our estimates have shown that at a low pulse repetition rate the thermal contact of the plasma with the reflector and strong dynamic loads are inevitable. The situation is aggravated by the excitation of resonance oscillations in the rocket body. These difficulties can be eliminated by using the method based on the merging of shock waves. Calculations and experiments [28] have confirmed the possibility of producing the stationary propulsion by using laser radiation with high laser pulse repetition rates. The method of scaling the output radiation power is presented in [10].

6. Matrix of reflectors

This matrix consists of N -element single reflectors, pulse-periodic radiation with a repetition rate of 100 kHz, pulse energy q and average power W_C . All elements of the matrix are very similar (Figure 7), radiation comes with the same parameters: $qm = q / N$, $W_m = W_C / N$. The matrix of reflectors creates a matrix of OPD, each one is stabilized by gas flux with velocity - V_{jm} . OPD's have no interactions in between. Elements structure of the matrix of reflectors could help find the solution for better conditions of gas flux penetration. In our case the number of reflectors was $N = 8$. Larger values of N are not reasonable.

The following estimations are valid for the boundary conditions: $W_C = 20$ MW ($W_m = 2.5$ MW), $f = 105$ Hz, $q = 200$ J ($q_m = 25$ J), $a_{rm} = 0.3$. Index 1 is for - $P_0 = 1$ atm. (Start of "Impulsar") and index 2 for $P_0 = 0.1$ atm. (end of regime).

Radius of cylinder for each reflector

$$R_{rm} = \frac{0.2R_{djm}}{\delta_m^{1/2}} = \frac{0.43(q_m/P_{j2m})^{1/3}}{\delta_m^{1/2}} = \frac{R_r}{N^{1/3}} = 15.5 \text{ cm}$$

Focus of reflector ~ 5 cm. The size of matrix ~ 90 cm. Additional pressure is:

$$\delta P_{m1} = 1.56 \text{ atm. and } \delta P_{m2} = 0.55 \text{ atm.}$$

Force acting on matrix:

$$F_{am1} = 100 \cdot 103 \text{ N, } F_{am2} = 35.6 \cdot 103 \text{ N.}$$

Specific force for each element of the matrix (for MW of average power):

$$J_{m1} \approx 4000 \text{ N/MW, } J_{m2} \approx 1500 \text{ N/MW.}$$

The velocities of gas flux in the reflectors of matrix:

$$V_{j1} = 2520 \text{ m/s, } V_{j2} = 5440 \text{ m/s}$$

Flight control in this case can be done by thrust change for the different elements of the matrix of reflectors. At the same time, such a configuration could be very helpful in the realization of efficient gas exchange in the area of breakdown behind of the reflectors (Figure 7).

Thus, an OPD can be stationary or move at a high velocity in a gaseous medium. However, stable SW generation occurs only for a certain relation between the radiation intensity, laser pulse repetition rate, their filling factor, and the OPD velocity. The OPD generates a QSW in the surrounding space if it is stationary or moves at a subsonic velocity and its parameters satisfy the aforementioned conditions. The mechanism of SW merging operates in various media in a wide range of laser pulse energies. The results of investigations show that the efficiency of the high repetition rate pulse-periodic laser radiation can be increased substantially when a QSW is used for producing thrust in a laser engine [13, 14].

7. Super long conductive canal for energy delivery

Powerful lasers are capable to create the spending channels of the big length which are settling down on any distances from a radiator. At relatively small energies of single

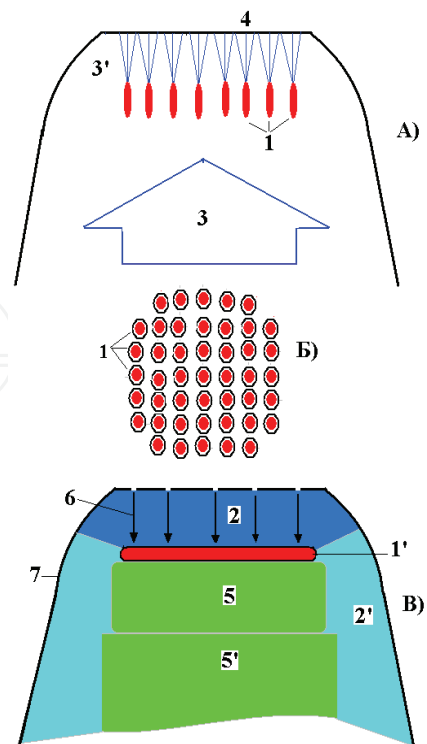


Fig. 7. "Impulsar" engine scheme based on QSW. A) Focusing system, B) – OPD matrix, creating flat QSW; B) Plasma created inhomogeneities; 1) OPD elements; 1') Model of OPD (Distance from 1' to 4: less 10 cm); 2) Flat QSW, $(P - P_0)/P_0 \approx 0.5 - 3$; 2') Radial QSW, $(P - P_0)/P_0 < 0.1$; 3) Main beam, $q \sim 100$ J; 3' – focused beams $q \sim 3-5$ J, creating QSW matrix; 4) Matrix of focusing elements and air injecting system; 5) OPD matrix of plasma decay; 5') OPD plasma turbulence ; 6) Gas flow; 7) Nozzle.

impulses the lengths of channels make about hundreds of meters. Since 1970 the successful attempts of their usage were undertaken for solution of problems of interception of lightning and blocking of overload waves on electric lines. The traditional lightning protection systems being used currently are not always in a position to ensure the desired level of efficiency. This stimulates the quest for new approaches to solve this problem. Laser protection against lightning is one of the most prospective trends that are being developed actively at present [29,30].

. While using this approach, it is assumed that the lightning discharge channel being developed is guided towards the conventional rod of the metal lightning rod along the plasma channel formed as a result of the laser induced breakdown of the atmosphere. This method is based on the concept of an active lightning rod, when a laser beam can be used for "triggering" and guiding a positive ascending leader from the tip of a lightning rod to a negatively charged thunderstorm cloud. It is expected that in contrast to the traditional approach, the use of laser spark will make it possible to control efficiently the very process of protection from lightning, ensure the selectivity of lightning capture, and provide safety of tall objects and large areas. Conductive canal in this case is about 10-15m long and main advantage of the approach is due to immediate appearance of laser produced prolongation of the lightning rod. But maximum length of the laser produced breakdown in the air was registered on the level of 100m and limited by optical method of laser energy delivery into the focal point. Where is the way to get conductive canal of much longer length?

The same goal to produce long conductive canal has ongoing French-German program "Teramobile", based on femto - second multi-photon lasers technology. But the goal is to get very long canal with very low level of electrical resistivity in comparison with canals produced by infrared laser radiation breakdown. The ionisation of air, produced by ultra-intense and ultra-short pulse can be put to use to channel bolts of lightning. As a "Teramobile" burst propagates it creates a sort of straight filament of ionised air, which should conduct electricity. If the laser were directed toward a dark and threatening thunderhead, it would trigger a lightning bolt that could be safely pushed away from doing harm. This capacity has already been demonstrated over a distance of a few meters only with a laboratory version of lightning, and tests on a more natural scale are limited by very high filaments resistivity. So what do we do with a mobile terawatt laser, if it is not good enough for the lightning control ? It can be used very effectively to study the propagation of intense laser light in the atmosphere, detect pollution, and control the parameters of fast objects in the space. Ultra - high intensity brings its own special qualities; it modifies significantly the index of refraction while it induces a focusing of the light beam along its path, the effect of the latter being to produce a self - guiding laser burst which can travel hundreds of meters. Another effect is that the luminous spectrum widens to yield a white laser whose light is composed of a wide range of wavelengths, which is important for a wide spectrum of applications.

There upon the well known program of creation of "Impulsar" represents a great interest, as this program in a combination with high-voltage high - frequency source can be useful in the solution of above mentioned problems. The principle of "Impulsar" operation can be shortly described as follows [31].

Jet draught of the offered device is made under influence of powerful high frequency pulse-periodic laser radiation. In the experiments the CO₂ laser and solid - state Nd YAG laser systems were used. Active impulse appears thanks to air breakdown (<30km) or to the breakdown of vapour of low-ionizable material saturated by nano - particles (dust plasma), placed on the board in the vicinity of the focusing mirror - acceptor of breakdown waves. With each pulse of powerful laser the device rises up, leaving a bright and dense trace of products with high degree of ionization and metallization by nano - particles after ablation. The theoretical estimations and experimental tests show that with already experimentally demonstrated figures of specific thrust impulse the lower layers of the Ionosphere can be reached in several ten seconds that is enough to keep the high level of channel conductivity with the help of high frequency high voltage generator.

The space around globe represents a series of megavolt class condensers created by Earth surface, the cloudy cover, various layers of ionosphere and radiating belts. With the help of supported by high - voltage source of trajectory trace of "Impulsar" it is possible to create a conductive channel of required length and direction. In process of the optical vehicle lifting and conductive channel following it, the breakdown characteristics of the interval with decreasing for 5 orders of magnitude (90 km) density considerably reduce, than the process must be prolonged by the expanding of micro-discharges net and develop as self - supported process in the external field of all studied interval. It is important to notice, that presence of such an orbital scale channel allows us also to perform a number of important experiments from the Earth surface as well as from space. Ball and bead lightning investigation is the most interesting application for the long conductive canal technology based on "Impulsar" due to the intriguing possibility for investigator to set up the stationary laboratory with variable boundary conditions for effective tests. Most likely, their nature is

multiple. It would appear that natural ball lightning may be not one phenomenon but many, each with similar appearance but with different mechanisms of origin, different stability criteria, and somewhat different properties dependent upon the atmosphere and the environment present at the time of the event.

Consideration of a large set of available applications of high power high repetition rate pulse-periodic lasers give us strong confidence to open on that basis a new horizons of instrumental space science and wide spectrum of very new and important applications.

8. Acknowledgments

The author would like to acknowledge the valuable contributions made to the "Impulsar" program by N.P.Laverov, S.N.Bagaev, B.I. Katorgin, Yu.M.Baturin.V.N. Tishchenko, G.N. Grachev, V.V. Kijko, Yu.S. Vagin, and A.G. Suzdal'tsev.

9. References

- [1] A. R. Kantrowitz *Astronautics and Aeronautics*, 10 (5), 74 (1972).
- [2] A. Pirry, M. Monsler, R. Nebolsine *Raket. Tekh. Kosmonavt.*, 12 (9), 112 (1974).
- [3] V. P. Ageev, A. I. Barchukov, F. V. Bunkin, V. I. Konov, A. M. Prokhorov, A. S. Silenok, N. I. Chapliev *Kvantovaya Elektron.*, 4, 2501, *Sov. J. Quantum Electron.*, 7, 1430 (1977).
- [4] W. Schall *Proc. SPIE Int. Soc. Opt. Eng.*, 4065, 472 (2000).
- [5] L. N. Myrabo, Yu. P. Raizer 2nd *Int. Symp. on Beamed Energy Propulsion*, Japan, p. 534.(2003)
- [6] V. E. Sherstobitov, N. A. Kalitievskiy, V. I. Kuprenyuk, A. Yu.Rodionov, N. A. Romanov, V. E. Semenov, L. N. Soms, N. V. Vysotina 2nd *Int. Symp. on Beamed Energy Propulsion* Japan, p. 296,(2003)
- [7] V.Hasson, F. Mead, C. Larson *III Int. Symp. on Beamed Energy Propulsion*, New York, p. 3
- [8] K. Mori, L. Myrabo *III Int. Symp. on Beamed Energy Propulsion* (Troy, New York, 2004) p. 155,(2004)
- [9] C. S. Hartley, T. W. Partwood, M. V. Filippelli, L. N. Myrabo, H. T. Nagamatsu, M. N. Shneider, Yu.P. Raizer *III Int. Symp. On Beamed Energy Propulsion*, Troy, New York, p. 499,(2004)
- [10] V. V. Apollonov, A. B. Egorov, V. V. Kiiko, V. I. Kislov, A. G. Suzdal'tsev *Kvantovaya Elektron.*, 33, 753, *Quantum Electron.*, 33, 753 (2003).
- [11] G. N. Grachev, A. G. Ponomarenko, A. L. Smirnov, V. B. Shulyat'ev *Proc. SPIE Int. Soc. Opt. Eng.*, 4165, 185 (2000)
- [12] V. N. Tishchenko, V. V. Apollonov, G. N. Grachev, A. I. Gulidov, V. I. Zapryagaev, Yu.G. Men'shikov, A. L. Smirnov, A. V. Sobolev *Kvantovaya Elektron.*, 34, 941, *Quantum Electron.*, 34, 941 (2004).
- [13] V. V. Apollonov, V. N. Tishchenko *Kvantovaya Elektron.*, 34, 1143, *Quantum Electron.*, 34, 1143 (2004)].
- [14] V. V. Apollonov, V. N. Tishchenko *Kvantovaya Elektron.*, 36, 763, *Quantum Electron.*, 36, 763 (2006).
- [15] G. N. Grachev, A. G. Ponomarenko, V. N. Tishchenko, A. L. Smirnov, S. I. Trashkeev, P. A. Statsenko, M. I. Zimin, A. A. Myakushina, V. I. Zapryagaev, A. I. Gulidov, V. M. Boiko, A. A. Pavlov, A. V. Sobolev *Kvantovaya Elektron.*, 36, 470, *Quantum Electron.*, 36, 470 (2006).

- [16] U.Bielesch, M. Budde, B. Freisinger, F. Ruders, J. Schafer, J. Uhlenbusch *Proc. ICPIG XXI* (Arbeitsgemeinschaft, Plasmaphysik APP-RUB, p. 253.(1993)
- [17] P. K. Tret'yakov, G. N. Grachev, A. I. Ivanchenko, V. I. Krainev, A. G. Ponomarenko, V. N. Tishchenko *Dokl. Akad. Nauk*, 336 (4), 466 (1994).
- [18] L. N. Myrabo, Yu. P. Raizer *AIAA Paper*, No. 94-2451 (1994).
- [19] V. Yu.Borzov, V. M. Mikhailov, I. V. Rybka, N. P. Savishchenko, A. S. Yur'ev *Inzh.-Fiz. Zh.*, 66 (5), 515 (1994).
- [20] G. N. Grachev, A. G. Ponomarenko, A. L. Smirnov, P. A. Statsenko, V. N. Tishchenko, S. I. Trashkeev *Kvantovaya Elektron.*, 35, 973, *Quantum Electron.*, 35, 973 (2005).
- [21] A. M. Prokhorov, V. I. Konov, I. Ursu, I. N. Mikheilesku *Vzaimodeistvie lazernogo izlucheniya s metallami* Interaction of Laser Radiation with Metals, Moscow: Nauka, (1988).
- [22] V. P. Korobeinikov *Zadachi teorii tochechnogo vzryva* Problems of the Theory of Point Explosion, Moscow: Nauka, (1985).
- [23] Yu. P. Raizer *Gas Discharge Physics* (Berlin: Springer, 1991; Moscow: Nauka, 1987).
- [24] V. N. Tishchenko, V. M. Antonov, A. V. Melekhov, S. A. Nikitin, V. G. Posukh, P. K. Tret'yakov, I. F. Shaikhislamov. *Pis'ma Zh. Tekh. Fiz.*, 22, 30 (1996).
- [25] V. V. Apollonov, V. N. Tishchenko. *Kvantovaya Elektron.*, 37 (8), 798, *Quantum Electron.*, 37 (8), 798 (2007).
- [26] F. V. Bunkin, A. M. Prokhorov. *Usp. Fiz. Nauk*, 119, 425 (1976).
- [27] S. N. Kabanov, L. I. Maslova, T. I. Tarkhova, V. A. Trukhin, V. T. Yurov. *Zh. Tekh. Fiz.*, 60, 37 (1990).
- [28] G. N. Grachev, V. N. Tishchenko, V. V. Apollonov, A. I. Gulidov, A. L. Smirnov, A. V. Sobolev, M. I. Zimin, *Kvantovaya Elektron.*, 37, 669, *Quantum Electron.*, 37, 669 (2007).
- [29] Apollonov V. V. *Optical engineering* 44(1) 2005,
- [30] Aleksandrov G.N., Ivanov V.L., Kadzov G.D., et al. *Elektrichestvo* (12), 47 (1980).
- [31] V.V.Apollonov, "Super long conductive canal for energy delivery", Proceedings of GCL/HPL Symposium, Sofia -2010, SPIE 7751.
- [32] V. V. Apollonov, "To the space by laser light", *Vestnik RANS* 1, (2008);
- [33] V.V.Apollonov, Patent RF "The conductive canal creation in nonconductive medium", № 2400005 от 20.05.09.



Laser Pulse Phenomena and Applications

Edited by Dr. F. J. Duarte

ISBN 978-953-307-405-4

Hard cover, 474 pages

Publisher InTech

Published online 30, November, 2010

Published in print edition November, 2010

Pulsed lasers are available in the gas, liquid, and the solid state. These lasers are also enormously versatile in their output characteristics yielding emission from very large energy pulses to very high peak-power pulses. Pulsed lasers are equally versatile in their spectral characteristics. This volume includes an impressive array of current research on pulsed laser phenomena and applications. *Laser Pulse Phenomena and Applications* covers a wide range of topics from laser powered orbital launchers, and laser rocket engines, to laser-matter interactions, detector and sensor laser technology, laser ablation, and biological applications.

How to reference

In order to correctly reference this scholarly work, feel free to copy and paste the following:

Victor Apollonov (2010). 'Impulsar': New Application for High Power High Repetition Rate Pulse-Periodic Lasers, *Laser Pulse Phenomena and Applications*, Dr. F. J. Duarte (Ed.), ISBN: 978-953-307-405-4, InTech, Available from: <http://www.intechopen.com/books/laser-pulse-phenomena-and-applications/impulsar-new-application-for-high-power-high-repetition-rate-pulse-periodic-lasers>

INTECH
open science | open minds

InTech Europe

University Campus STeP Ri
Slavka Krautzeka 83/A
51000 Rijeka, Croatia
Phone: +385 (51) 770 447
Fax: +385 (51) 686 166
www.intechopen.com

InTech China

Unit 405, Office Block, Hotel Equatorial Shanghai
No.65, Yan An Road (West), Shanghai, 200040, China
中国上海市延安西路65号上海国际贵都大饭店办公楼405单元
Phone: +86-21-62489820
Fax: +86-21-62489821

© 2010 The Author(s). Licensee IntechOpen. This chapter is distributed under the terms of the [Creative Commons Attribution-NonCommercial-ShareAlike-3.0 License](https://creativecommons.org/licenses/by-nc-sa/3.0/), which permits use, distribution and reproduction for non-commercial purposes, provided the original is properly cited and derivative works building on this content are distributed under the same license.

IntechOpen

IntechOpen